Applied and Environmental Microbiology, June 2011, p. 3644–3652 Vol. 77, No. 11
0099-2240/11/$12.00 doi:10.1128/AEM.02656-10
Copyright © 2011, American Society for Microbiology. All Rights Reserved.

Dynamics of Flagellum- and Pilus-Mediated Association of *Pseudomonas aeruginosa* with Contact Lens Surfaces[▽]

Victoria B. Tran,[1] Suzanne M. J. Fleiszig,[2,3,4]* David J. Evans,[2,5] and Clayton J. Radke[1,3]

Chemical and Biomolecular Engineering Department, University of California, Berkeley, California 94720[1]; School of Optometry, University of California, Berkeley, California 94720[2]; Graduate Group in Vision Science, University of California, Berkeley, California 94720[3]; Graduate Groups in Plant and Microbial Biology and Infectious Disease and Immunity, University of California, Berkeley, California 94720[4]; and College of Pharmacy, Touro University—California, Vallejo, California 94592[5]

Received 12 November 2010/Accepted 6 April 2011

Flagella and pili are appendages that modulate attachment of *Pseudomonas aeruginosa* to solid surfaces. However, previous studies have mostly reported absolute attachment. Neither the dynamic roles of these appendages in surface association nor those of attachment phenotypes have been quantified. We used video microscopy to address this issue. Unworn, sterile, soft contact lenses were placed in a laminar-flow optical chamber. Initial lens association kinetics for *P. aeruginosa* strain PAK were assessed in addition to lens-surface association phenotypes. Comparisons were made to strains with mutations in flagellin (*fliC*) or pilin (*pilA*) or those in flagellum (*motAB*) or pilus (*pilU*) function. PAK and its mutants associated with the contact lens surface at a constant rate according to first-order kinetics. Nonswimming mutants associated ~30 to 40 times slower than the wild type. PAK and its *pilA* mutant associated at similar rates, but each ~4 times faster than the *pilU* mutant. Lens attachment by wild-type PAK induced multiple phenotypes (static, lateral, and rotational surface movement), each showing only minor detachment. Flagellin (*fliC*) and flagellar-motility (*motAB*) mutants did not exhibit surface rotation. Conversely, strains with mutations in pilin (*pilA*) and pilus retraction (*pilU*) lacked lateral-surface movement but displayed enhanced surface rotation. Slower surface association of swimming-incapable *P. aeruginosa* mutants was ascribed to lower convective-diffusion-arrival rates, not to an inability to adhere. Flagellum function (swimming) enhanced lens association, attachment, and rotation; hyperpiliation hindered lens association. *P. aeruginosa* bound through three different adhesion sites: flagellum, pili, and body. Reduction of bacterial attachment to contact lenses thus requires blockage of multiple adhesion phenotypes.

Pseudomonas aeruginosa is a ubiquitous bacterium notorious for causing serious infections in the airways, urinary tract, and cornea (8, 30, 36). Healthy corneas are inherently resistant to *P. aeruginosa* infection (43, 47) but appear more susceptible with soft-contact-lens wear, especially overnight or extended-wear modalities (25, 42). Since most *P. aeruginosa* corneal and other infections are difficult to treat, there is an urgent need to understand infection pathogenesis and develop novel methods of treatment and prevention (12, 61). One possible mitigating measure against infection is the reduction/prevention of bacterial adhesion to tissues and medical devices, including the contact lens (9, 61).

P. aeruginosa adhesion to substrates, including soft-contact lenses, has been studied extensively (5, 23, 28, 41, 54, 55, 58), and roles for pili and flagella have been documented (15, 17, 45, 46). Pili are hairlike appendages on the surface of *P. aeruginosa* and are responsible for surface lateral motility (also known as twitching motility) (38, 40). Some studies argue that pili are responsible for surface attachment, while others refute that role (13, 17, 19, 20, 46, 52, 62). Some strains of *P. aeruginosa* also exhibit a polar flagellum that allows the bacteria to swim (49). Flagella are argued by some to provide only a means for transport to a surface (15, 27, 45). Conversely, other investigators suggest that flagellin, the structural unit of the flagellum, is an adhesive factor that permits surface binding (1, 15, 22, 32, 45, 49).

Many measurements of bacterial uptake expose a fixed aqueous concentration of bacteria to a surface in a poorly defined flow field for a fixed time and count the number of viable bacteria after "loosely" held material are washed away (4, 11, 18, 48). In such studies, the rate of bacterial arrival to the surface, the fraction of those arriving that stick, and the uptake kinetics cannot be quantified. Moreover, bacteria in some surface adhesion studies have been treated as inanimate colloids instead of as living organisms (5–7, 15, 23). It is well known that bacteria attached to solid surfaces exhibit motion (37, 39, 49, 51, 52, 56). Due to the limitations of many current assays, little mechanistic information is available on the roles of bacterial appendages in surface association.

To understand the mechanism(s) of initial bacterial uptake to soft contact lenses and the underlying roles of appendage adhesins, we utilized video microscopy in a transparent microflow cell. The optical flow chamber was specially designed to provide well-defined laminar parabolic flow across the lens, allowing calculation of the rate of transport to the surface. Our

* Corresponding author. Mailing address: School of Optometry, University of California, Berkeley, CA 94720. Phone: (510) 643-0990. Fax: (510) 643-5109. E-mail: fleiszig@berkeley.edu.
▽ Published ahead of print on 15 April 2011.

hypothesis was that *P. aeruginosa* binds to a soft contact lens in multiple ways that manifest as different attachment phenotypes. To distinguish the relative roles of pili and flagella in surface association, we quantified the uptake kinetics and phenotypes of *P. aeruginosa* pilin and flagellin structural and functional mutants by time lapse and real-time phase-contrast microscopy.

MATERIALS AND METHODS

Bacterial strains and culture conditions. *P. aeruginosa* strain PAK and its motility mutants, PAKΔ*fliC* and PAKΔ*motAB*, were kindly provided by Stephen Lory (Harvard Medical School). PAKΔ*fliC* lacks flagellin, hence the entire flagellum, and thus is unable to swim (14). PAKΔ*motAB* has a flagellum, but not a functional motor, and also cannot swim (14). *P. aeruginosa* strain PAK and its twitching motility mutants PAKΔ*pilA* and PAKΔ*pilU* were also studied. The pilus parent-mutant set was previously constructed and characterized by John S. Mattick (University of Queensland, Australia) (59, 60) and was kindly provided by Joanne Engel (University of California, San Francisco, CA) with John S. Mattick's permission. PAKΔ*pilA* is a nonpiliated, isogenic mutant and thus is also twitching motility defective (59). PAKΔ*pilU* has pili but is unable to retract them, and thus is also twitching motility negative. Indeed, PAKΔ*pilU* is hyperpiliated from the expression of paralyzed fully extended pili (60).

Bacteria were recovered from frozen stocks by growth on Trypticase soy agar at 37°C overnight. Single colonies were inoculated into 12 ml of a modified Mian's minimal medium: sodium phosphate monobasic monohydrate (7.5 mM), potassium phosphate anhydrous (16.8 mM), magnesium sulfate heptahydrate (10 mM), sodium nitrate (23.5 mM), and sodium acetate (10 mM) (reagent grade; Fisher) in ultrapure water and filter sterilized (29). Except for sodium acetate, all reagents were reagent grade from Sigma (St. Louis, MO). All were used without further purification. Modified Mian's minimal medium was employed since it is transparent, chemically well defined, and supports bacterial growth at a lower rate than nutrient-rich media. Importantly, the low nutrient content of Mian's medium more closely mimics the low nutrient content of contact lens care solutions. Bacteria were grown in a rotary shaker at 37°C and 250 rpm until the culture reached an optical density at 650 nm (OD_{650}) of 0.15, corresponding to a late-exponential growth phase. The resulting culture was then diluted to the desired concentration of $\sim 5 \times 10^6$ CFU/ml by diluting 6 ml of the culture into 210 ml of fresh modified Mian's minimal medium and used immediately for attachment assays. Bacterial concentrations were confirmed by viable-cell counts.

In some experiments, *P. aeruginosa* was fluorescently labeled with Alexa Fluor 546 carboxylic acid succinimidyl ester (Molecular Probes) as previously described (57), but with slight modification. Briefly, a single colony of bacteria was inoculated into 5 ml of Trypticase soy broth (TSB) and grown overnight (37°C, with shaking at 250 rpm). One hundred microliters of that culture was then used to inoculate 10 ml of fresh TSB. The culture was then grown for 4.5 h (37°C, with shaking at 250 rpm), washed by centrifugation at 2,000 relative centrifugal force (RCF) units ($2{,}000 \times g$) for 10 min, and recovered and resuspended in sterile phosphate-buffered saline (PBS) (10 ml; pH 7.4; laboratory grade; Sigma). The wash step was repeated twice. Alexa Fluor 546 carboxylic acid succinimidyl ester was added, and the culture was incubated for 1 h in the dark with gentle shaking. Unreacted dye was removed by washing as described above. The labeled bacteria were then suspended in 1 ml of Mian's minimal medium.

Parallel-plate flow chamber. As illustrated in Fig. 1, bacterial interactions with a soft-contact-lens surface were studied in a transparent, parallel-plate laminar-flow chamber designed to rest on a phase-contrast microscope. The flow chamber provided fully developed laminar flow across the soft contact lens. Bacteria were thereby introduced to the lens surface at a constant and known surface shear rate. The chamber frame was constructed of G10 fiberglass epoxy resin. A standard 3- by 1-inch glass microscope slide (Fisher Scientific) served as the chamber top, while the bottom was a 60- by 24-mm glass coverslip (Fisher Scientific). The soft contact lens was mounted to the cover glass 35 mm downstream of the chamber entrance and was held in place with a 60- by 24-mm, 0.25-mm-thick G10 fiberglass epoxy resin sheet with a 5-mm-diameter aperture, allowing for lens exposure to the flow stream. New cover glass and microscope slides were used for each experiment. Flow entered and exited the flow cell via 0.125-cm-diameter ports. A 2-mm baffle near the flow chamber entrance evenly distributed the flow into a parabolic profile. One-dimensional parabolic flow at the location of the soft contact lens was confirmed with Multiphysics simulations (Comsol).

For each surface assay, a new O_2Optix (Balafilcon A; CIBA Vision, Duluth, GA) silicone-hydrogel lens was soaked in sterile PBS, pH 7.4 (Sigma) for 2 days to remove blister pack additives, e.g., surfactants and preservatives. O_2Optix lenses were chosen for their relatively uniform plasma surface coating (33, 35), as verified by atomic force microscopy (data not shown). A 10-mm-diameter circular section was cut from the lens using a corer and was mounted in the flow chamber such that the bacterial suspension flowed past the lens's posterior side. The posterior side of the lens was chosen for examination since under contact lens wear, it is the side in closest contact with the cornea. Before the surface assay with phase-contrast microscopy, the flow cell was primed with modified Mian's minimal medium while the pump (Pharmacia LKB-Pump P-500) and all lines entering the flow cell were primed with the freshly prepared bacterial suspension. During bacterial deposition, a flow rate of 210 ml/h was set, corresponding to a surface shear rate of 0.2 s^{-1}. This low shear rate was chosen to provide a well-defined and reproducible rate of mass transfer to the lens surface. In addition, entrained, nonadherent bacteria drifted past the contact lens. As described below, these bacteria were counted as part of those associated with the surface. Each attachment assay lasted 1 to 2 h and was conducted at an ambient temperature of ~22°C. There was no detectable bacterial growth during that time frame.

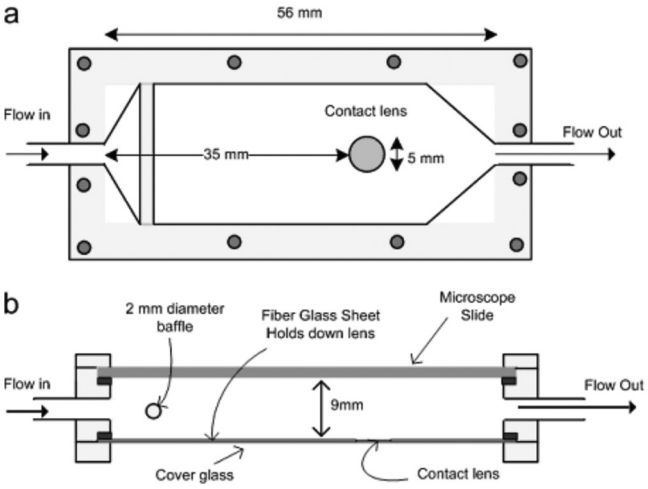

FIG. 1. Plan (a) and side (b) views of the parallel-plate flow chamber for bacterial adhesion assays. A baffle at the entrance of the flow chamber more uniformly distributes the bacteria.

For bacteria labeled with Alexa Fluor 546 carboxylic acid, 20 μl of fluorescently labeled bacterial suspension was added to an Attofluor cell chamber (Molecular Probes) containing a mounted 25-mm-diameter glass coverslip and 980 μl of fresh Mian's medium and viewed under fluorescence microscopy.

Microscopy. In each experiment, *P. aeruginosa* adhesion was visualized by time lapse or real-time video phase-contrast microscopy (Olympus IX70). To assess the rate of bacterial surface association, a 40× objective was focused through the contact lens onto its posterior side (total magnification, ×400). Images were captured with a black-and-white camera (Hamamatsu ORCA ER charge-coupled device [CCD]) and subsequently magnified and displayed digitally on a computer screen. Images were captured every 20 s with Volocity 4.0 imaging software. The number of bacteria associated with the surface of the lens in each captured image was quantified with Image J software (NIH). Bacteria were considered associated if they were within focus with the contact surface. Thus, all bacteria located within about 4 μm from the surface, the depth of focus of the microscope, were counted. Sequential video frames were analyzed for the number of bacteria associated with the surface over a 1- to 2-h period. The rate of bacterial association with the contact lens surface was scaled using a 1-mm^2 viewing area. As determined by viable-cell counting, each bacterial suspension had a somewhat different concentration. Hence, the rate of surface association was also scaled linearly to the nominal bulk bacterial concentration of 5×10^6 CFU/ml.

For experiments studying attachment phenotypes, phase-contrast microscopy with ×600 magnification was used. An analog camera captured bacterial behavior at the contact lens surface in real time. EyeTV (Elgato) converted the analog signal to digital for compression in QuickTime video. One hour after bacteria were detected at the contact lens surface, a 1-min interval of video was reviewed and examined for distinct phenotypes. For fluorescence microscopy experiments,

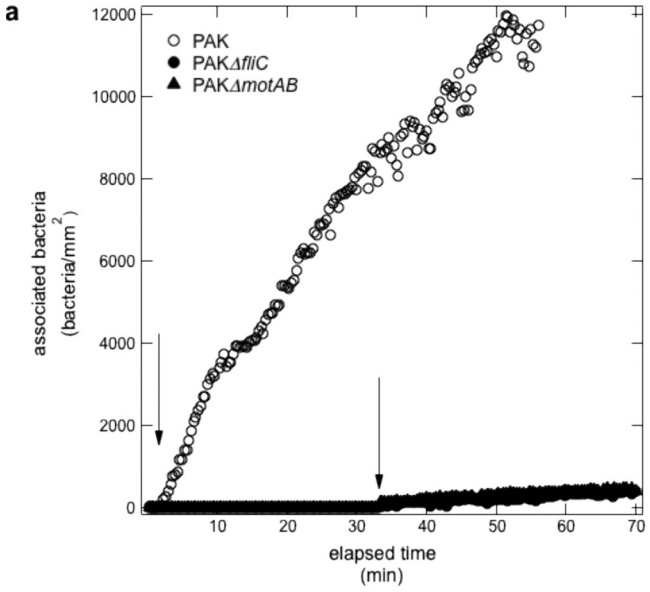

FIG. 2. (a) Number per unit surface area of PAK (open circles), PAKΔ*fliC* (filled circles), and PAKΔ*motAB* (filled triangles) bacteria associated with the contact lens surface as a function of time. Data for PAKΔ*motAB* (filled triangles) are hidden by those for PAKΔ*fliC* (filled circles). Arrows indicate the time of arrival of the bacteria to the lens. (b) Rates of surface association from slopes of the linear regression in panel a. The asterisk indicates that the *P* value is less than 0.05 for comparison to the wild type.

the bacteria were viewed through a rhodamine filter at ×600 or ×1,000 total magnification. Images were captured with a black-and-white Hamamatsu ORCA ER CCD camera using Volocity 4.0 imaging software at a minimum of 9 frames/s. They were subsequently magnified and displayed digitally on a computer screen.

Statistics. All rate and phenotype distribution data are reported as means ± standard deviations. Experiments were repeated at least three times. Student's *t* test was used to determine the statistical significance of differences between two groups, with *P* values of <0.05 considered significant.

RESULTS

Swimming motility and association kinetics. Fig. 2a shows the number of bacteria per unit surface area associated with the contact lens as a function of time for PAK and its structural and functional flagellum mutants, PAKΔ*fliC* and PAKΔ*motAB*. PAKΔ*fliC* has no flagellum. To investigate the role of operative versus nonoperative flagella in surface association, we also studied PAKΔ*motAB*. This mutant has a flagellum but lacks a functional motor apparatus and, thus, cannot swim (14). Uptake data for PAKΔ*fliC* and PAKΔ*motAB* were indistinguishable in Fig. 2a. Dark vertical arrows denote the first arrival of bacteria to the contact lens surface. Wild-type (wt) PAK exhibited a short lag of ~2 to 5 min before bacteria were observed at the surface. Swimming-deficient mutants, PAKΔ*fliC* and PAKΔ*motAB*, however, exhibit a much longer lag of ~30 min. After arrival, all strains accumulated linearly in time at the surface. The slope of the kinetic uptake curve gave the rate of association with the surface that, in all cases, was constant over the time range studied. As summarized in Fig. 2b, different strains clearly exhibited much different rates of association. The surface uptake rate for PAKΔ*motAB* (filled triangles) was nearly the same as that for PAKΔ*fliC* (filled circles). Wild-type PAK, however, associated with the soft contact lens (SCL) surface ~30 to 40 times faster than its nonswimming capable mutants. Separate uptake experiments with another *P. aeruginosa* strain (PAO1) similarly demonstrated a linear increase in time and 30- to 40-times-faster association of motile bacteria than nonswimming capable mutants (data not shown). We conclude that the drastically lower association rates observed in Fig. 2 for the flagellum mutants reflect an inability to swim rather than increased attachment via the flagellum in the wild-type strain.

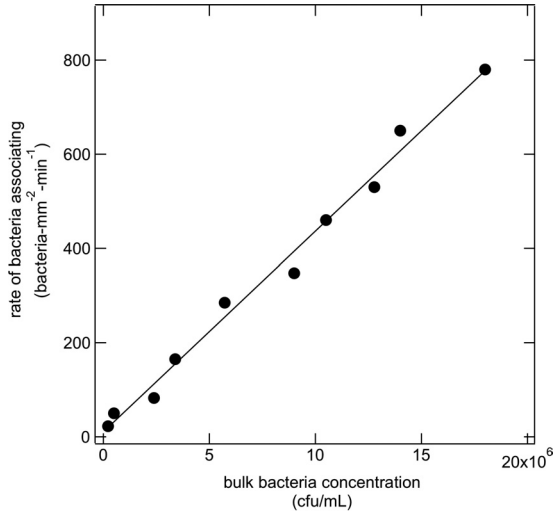

FIG. 3. Rates of association of wild-type PAK bacteria with the contact lens surface as a function of bulk bacterial solution concentration.

As shown in Fig. 3 for a 100-fold range of concentrations (2×10^5 to 2×10^7 CFU/ml), PAK obeys a linear increase of association rate with increasing concentration. If we let Γ denote the number of bacteria associated with the surface per unit area, then our uptake rate observations mean as follows:

$$d\Gamma/dt = kC \quad (1)$$

where *t* is time, *C* is the bulk concentration of bacteria, and *k* is a first-order rate constant. Since *k* and *C* are constant,

integration of equation 1 explains the straight-line increase in transient uptake seen in Fig. 2a for wt PAK and its motility mutants. Also explained is the observed linear increase in rate with bacterial concentration. Equation 1 holds only for dilute bacterial suspensions at early time points where surface coverage is minimal. For a bacterial mean size of ~1 μm, we calculate that only 2 to 4% of the contact lens surface was covered by wild-type PAK after 1 h. These results suggest that the bacteria arrived and associated with the surface uninfluenced by the presence of other bacteria. Further, if a significant number of bacteria initially adhered to the surface and then detached, association rates in Fig. 2 must decline in time; equation 1 is no longer valid. Since this is not the case, we conclude that detachment is minimal. Consequently, bacterial detachment rates are low at the low surface coverages studied. Further, washout of wild-type PAK by Mian's medium (containing no bacteria) after 1 h of loading demonstrated little decline in surface coverage (data not shown). This conclusion holds for the imposed 0.2 s^{-1} shear rate. We have not ascertained whether adhered bacteria detach under the higher shear rates of 1,000 s^{-1} typical of on-eye contact lens motion or if they detach due to phenotype changes after longer times.

Pili and association kinetics. Pili are often implicated as a mediator for bacterial attachment (13, 19, 20, 46). Consequently, if pili are removed, a lower rate of surface association is anticipated. A pilin mutant, PAKΔ*pilA*, was studied to determine the possible influence on attachment rate occurring when pili are lacking. Kinetics of association to the soft contact lens for PAKΔ*pilA* and wild-type PAK are compared in Fig. 4. No significant difference in the rate of bacterial association with the contact lens surface was seen.

We also studied PAKΔ*pilU*, which has pili but lacks the ability to retract them and, thus, cannot participate in surface-associated twitching motility. The rate of association of PAKΔ*pilU* in Fig. 4 was only 25% that of wild-type PAK or the pilin-deficient mutant PAKΔ*pilA*. The three bacterial strains in Fig. 4 are capable of swimming; they all reached the contact lens surface within minutes of the start of the experiment. Thus, lower association rates for PAKΔ*pilU* were not due to lower surface arrival rates but rather to an adsorption barrier to binding.

Association phenotypes. Video phase-contrast microscopy was used to observe the behavior of individual wild-type PAK bacteria associating with the contact lens surface. Figure 5 pictures the 5 different attachment phenotypes expressed by the PAK population. One group appeared to be "tethered" to the lens surface (Fig. 5a); these bacteria rotated randomly about a fixed point, as documented in Fig. 6a. The rotation phenotype is similar to that documented by Toutain et al. (56). Another fraction of bacteria remained fixed at the contact lens surface and did not exhibit observable movement (Fig. 5b). Some bacteria appeared attached to the lens surface but moved slowly along, even against the flow of fluid (Fig. 5c), as confirmed in Fig. 6b. Some bacteria approached the surface but did not stop and attach over the 1-min observation period (Fig. 5d). These nonattached bacteria either drifted with the flow stream (for swimming-deficient mutants) or swam randomly near the surface, including against the flow (for swimming bacteria). Nonattached bacteria were still considered surface associated because they were close enough to the lens surface to be interacting with it. Finally, small numbers from each of these classes detached and left the surface (Fig. 5e). Some of the phenotype classifications in Fig. 5 bear resemblance to those of Singh et al. (50), who designated fixed, stationary bacteria as squatters, laterally moving bacteria as ramblers, and detaching bacteria as flyers.

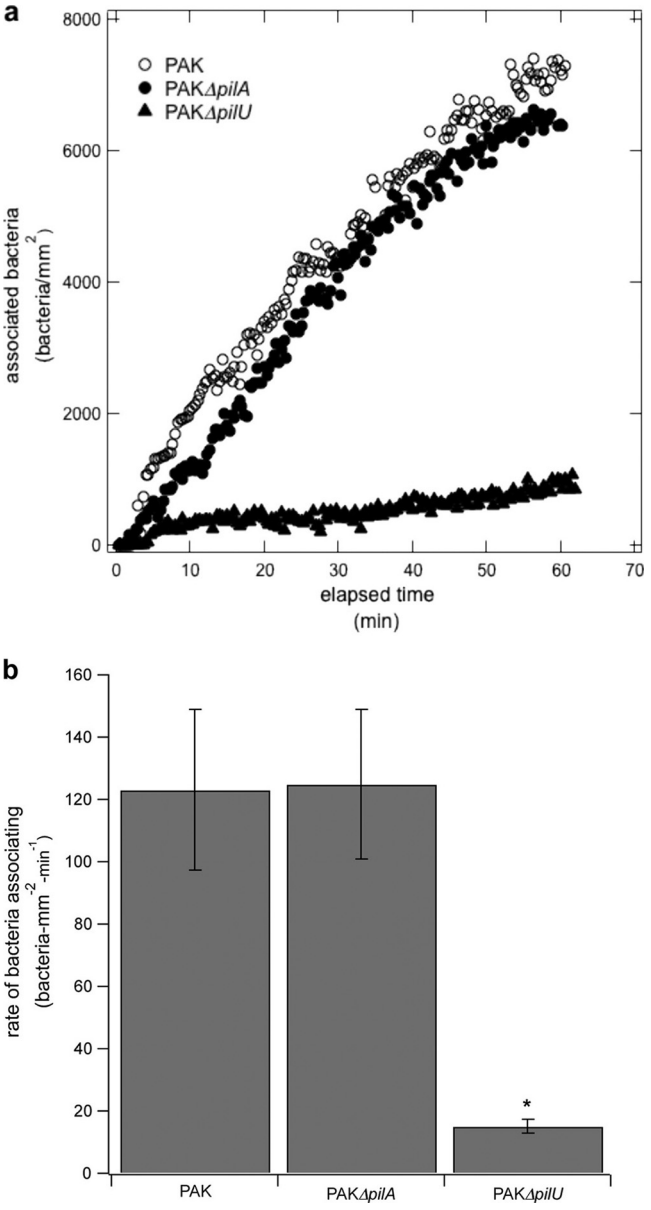

FIG. 4. (a) Number per unit area of PAK (open circles) bacteria and its pilus mutants, PAKΔ*pilA* (filled circles) and PAKΔ*pilU* (filled triangles), associated with the contact lens surface as a function of time. (b) Corresponding rates of surface association from slopes of the linear regression in panel a. The asterisk indicates that the *P* value is less than 0.05 for comparison to the wild type.

P. aeruginosa flagella can be directly viewed when the bacteria are labeled with Alexa Fluor 546 carboxylic acid. Wild-type PAK bacteria were seen attaching to a glass coverslip surface, and at times rotating while attached to the surface, similar to that seen by phase-contrast microscopy of the bac-

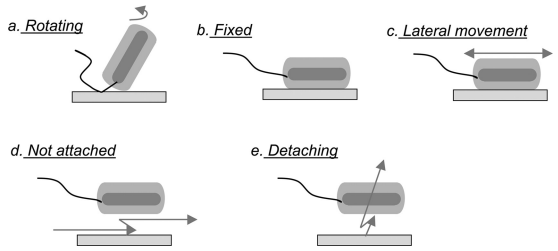

FIG. 5. Schematic of five surface association phenotypes. Dark gray corresponds to the bacterial body. Light gray represents the bacterial pilin. Phenotypes a to c adhered to the surface. Phenotype d did not. As discussed in the text, phenotypes a and d each exhibited two subclasses.

teria attached to the soft contact lens. Figure 7a to d and e to h reveal that the rotational phenotype displayed at least two distinct subpopulations. Figure 7a to d show that the wild-type bacteria adhered to the glass surface via their flagella and rotated their body while their flagella remained fixed. Additionally, bacteria attached to the glass coverslip and rotated both body and flagellum in concert, as shown in Fig. 7e to h. Here, the attachment point was on the body since the flagellum rotated in tandem.

To determine whether bacteria rotate when not attached by pili, PAKΔ*pilA* was fluorescently labeled. Figure 7i to l show a pilin mutant attached to the coverslip surface by its flagellum with the body rotating, similar to wild-type PAK in Fig. 7a to d. Similar to wild-type PAK in Fig. 7e to h, the PAKΔ*pilA* mutant in Fig. 7m to p also bound to the glass surface and rotated its body and flagellum in tandem. Thus, PAKΔ*pilA* bound to the surface and exhibited a rotational phenotype while attached to a point on its body, even though the bacterium has no pili.

Distribution of association phenotypes. Video microscopy allowed observation of not only the 5 association phenotypes but also the fraction of bacteria expressing each phenotype. Figure 8 illustrates results for wild-type PAK and its swimming-motility mutants, PAKΔ*fliC* and PAKΔ*motAB*. For wild-type PAK, over 95% of the individual bacteria associated with the contact lens surface were adhered. Most of these were fixed and remained stationary. A small fraction of the adhered bacteria rotated; a more substantial portion moved laterally (i.e., twitched). Less than 5% of surface-associated bacteria detached over the 1-min observation period. A small but measureable fraction of wild-type bacteria did not attach at all and appeared to swim randomly along the contact lens surface. The linear uptake kinetics in Fig. 2a and the distribution of surface phenotypes in Fig. 8 are in concert: wild-type PAK binds to the surface at this time point with minimal desorption.

For the Δ*fliC* flagellum mutant, no bacteria were observed to rotate on the lens surface. Similar findings were seen for the Δ*motAB* mutant. Loss in swimming motility removed the rotational phenotype. Consequently, surface rotation demands an active flagellum. Notably, PAKΔ*motAB* showed a significant fraction of entrained bacteria associating with, but not binding to, the contact lens surface.

Figure 9 presents analogous results for phenotype distributions of wild-type PAK and its pilus mutants, PAKΔ*pilA* and PAKΔ*pilU*. As expected, the lack of pili on PAKΔ*pilA* and the lack of pilus retraction on PAKΔ*pilU* completely eliminated

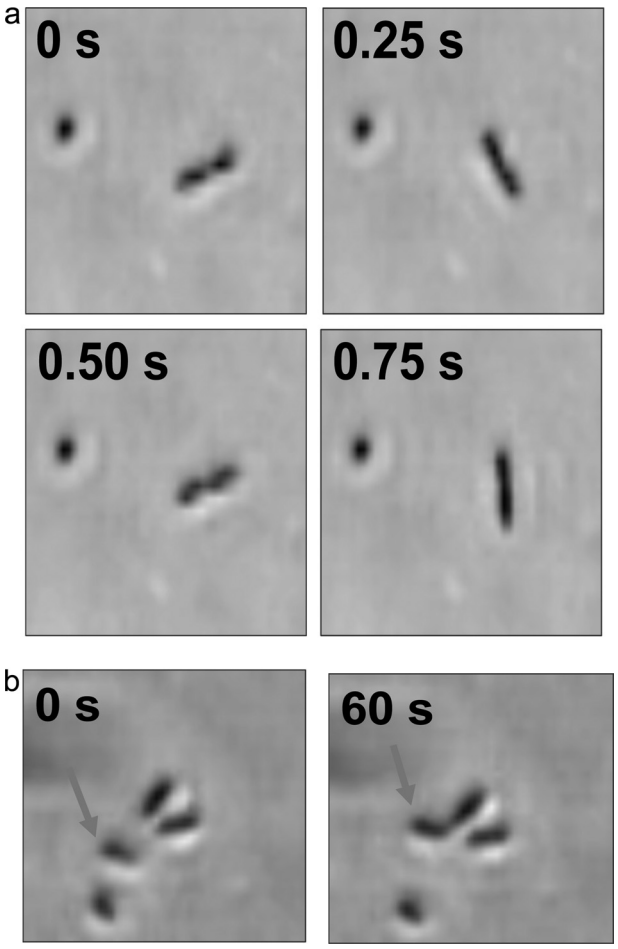

FIG. 6. Time lapse phase-contrast images of bacteria: rotating (a) and moving laterally (twitching) (b). Rotating bacteria appear tethered to the contact lens by a single point and spin clockwise around that point at least once in 60 s. Laterally moving bacteria move at least one bacterial body width while remaining at the contact lens surface. Flow direction was from left to right.

lateral movement. Upon loss of twitching motility, the fraction of rotating bacteria increased ~3-fold compared to the level for wild-type bacteria, with the remaining phenotype populations remaining about the same. In all cases, the fraction of pilus mutants not attached or detaching was small.

DISCUSSION

Our data show that wild-type *Pseudomonas aeruginosa* strain PAK and each of its structural and functional flagellum and pilus mutants initially associate with a soft contact lens surface by linear uptake kinetics, as seen in Fig. 2a and 4a. Linear uptake kinetics indicates a constant rate of bacterial accumulation at the surface. Rates of surface association also increased linearly with bacterial concentration, revealing that bacteria arrive and interact with the surface individually. Although constant arrival rates were found for all bacteria in this study, Fig. 2b and 4b reveal that nonswimming mutants accumulated at an ~30- to 40-times-lower rate. In our laminar flow chamber, bacteria in dilute suspension reached the focal depth

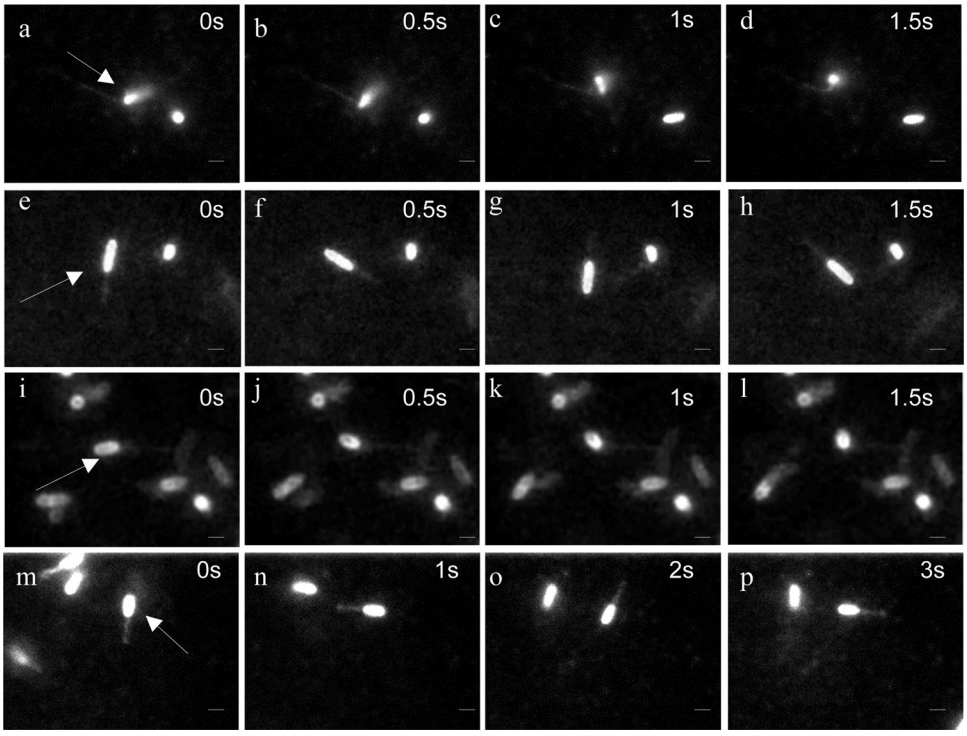

FIG. 7. Fluorescence microscopy. (a to d) Rotation of the wild-type PAK body while attached to coverslip by its fixed flagellum; (e to h) PAK attached to a coverslip at a point with both body and flagellum rotating together; (i to l) PAKΔ*pilA* attached to the coverslip by its flagellum; and (m to p) PAKΔ*pilA* attached to the coverslip at a point on its body, with both the body and the flagellum rotating together.

of the contact lens surface by convective diffusion from an axial, parabolic velocity field to a sparsely covered surface. These conditions suggest arrival to the surface according to Lèvêque theory (31, 34, 44). In this situation, the ratio of association rates scales by the ratio of bacterial diffusion coefficients, each raised to the 2/3 power (i.e., $D^{2/3}$). Several studies have shown that *P. aeruginosa* swimming motility is correctly modeled as a random walk with an effective diffusion coefficient on the order of $\sim 10^{-6}$ cm^2/s (2, 3). To estimate the effective diffusion coefficient of the nonswimming PAK mu-

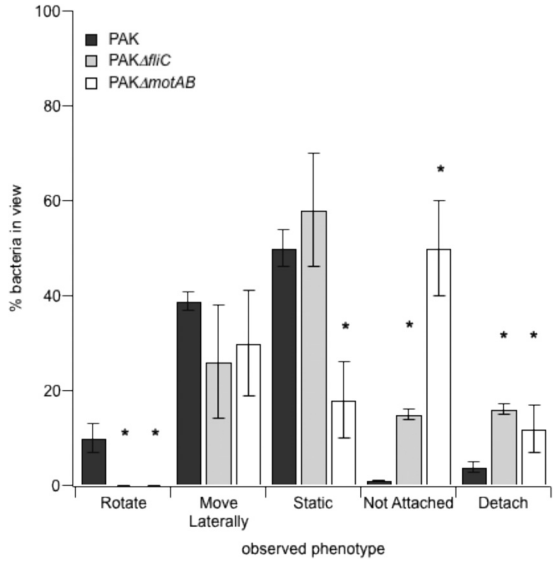

FIG. 8. Distribution of surface association phenotypes for wild-type PAK and its swimming-motility mutants. Typical error bars are shown. The asterisk indicates that the *P* value is less than 0.05 for comparison to the wild type.

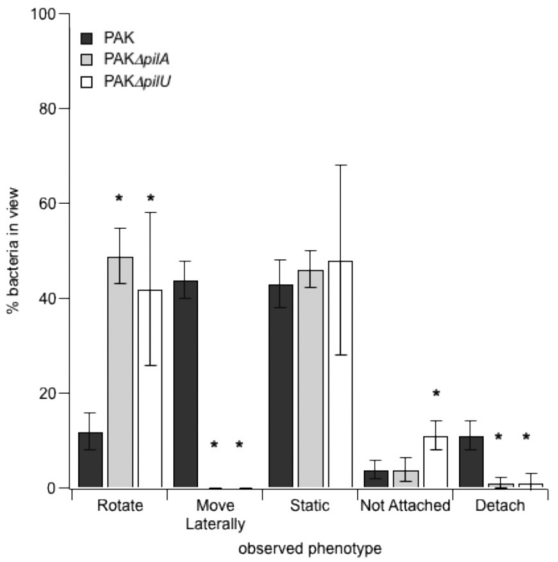

FIG. 9. Distribution of surface association phenotypes for wild-type PAK and its pilus mutants. Typical error bars are shown. The asterisk indicates that the *P* value is less than 0.05 for comparison to the wild type.

tants, we adopted the Stokes-Einstein theory of Brownian motion, $D = k_bT/6\pi\mu r_0$, where k_b is Boltzmann's constant, T is absolute temperature, μ is the solution viscosity, and r_0 is $a/ln(2a/b)$, with a half the length of the bacterium (0.5 μm) and b half the width of the bacterium (0.25 μm) (3, 15). We thus estimate the diffusion coefficient of the nonswimming bacteria as 6×10^{-9} cm^2/s. When these values are adopted in the Lèvêque theory, the ratio of arrival rates at the surface for the swimming strains to those for the nonswimming strains is about 30, in good agreement with the experimental data. This result indicates that PAK association with the SCL surface is governed by convective diffusion.

The significantly smaller diffusion coefficient of the nonactive flagellum mutants also explains why they do not first appear at the contact lens surface until about 0.5 h after the motile strains first appear. This is an important finding since the rate of bacterial uptake to a surface, such as in Fig. 2a and 4a, cannot be correlated with the ability to adhere to the surface. Although PAKΔ*fliC* arrived at the surface much slower than did wild-type PAK, Fig. 8 reveals that the fractions of bacteria bound to the surface after 1 h are similar for both wt PAK and PAKΔ*fliC*. The nonmotile bacteria simply required more time to reach the same surface coverage than the motile wild type.

Since rates of bacterial approach to a surface are influenced by convective diffusion, different apparatus assess different uptake kinetics and the relative role(s) of bacterial factors. Thus, bacterial uptake to a surface studied in a stagnant cell is slower than that studied in a flow cell. Using a microtiter plate assay under an observation time frame of hours, O'Toole and Kolter (45) found that flagella and pili are required for the initiation of biofilm formation. However, Klausen et al. (27), using a flow cell under a time frame of days, refute that finding. To distinguish phenotype binding mechanisms and strengths, surface adhesion studies must account quantitatively for the role of solution transport.

Figure 4a demonstrates that pili are not required for binding, since PAKΔ*pilA* accumulated at the same rate as wild-type PAK. PAKΔ*pilU* also can swim and, hence, should arrive to the surface at the same rate as did the *pilA* mutant. However, we and others (10, 13, 17, 24) find that surface association is small for hyperpiliated mutants of *P. aeruginosa*. Comolli et al. (13) proposed that twitching motility is required for binding and that PAKΔ*pilU*'s lack of pilus retraction precludes twitching and, thus, prevents binding. Since pili were not required here for initial adhesion to an SCL, we hypothesized, in agreement with Fletcher et al. (17), that hyperpiliation sterically hinders binding. Hyperpiliated bacteria are able to swim away and not accumulate at the contact lens surface.

If the nonattached mutant had no flagellum or if the flagellum was disabled, then the motion of nonattached bacteria was entrainment in the flow stream. For the disabled mutant, PAKΔ*motAB*, the fraction of entrained bacteria was almost 50%, indicating that despite being at the surface, many of the bacteria were unable to bind. It is also possible that like the hyperpiliated PAKΔ*pilU*, a paralyzed flagellum prevents adhesion by steric hindrance.

Within the attached class, bacteria may rotate, either about the body or about the flagellum (rotate), translate laterally along the surface by twitching (move laterally), attach stationary (fixed), and desorb (detach). Only bacteria with active flagella rotated on the surface. Rotation was either about a point on the body or on the flagellum. We did not observe rotation upon pilus attachment. Rotation about the body does, however, signify point attachment rather than multiple attachment locations along the bacterial body. Attachment to the contact lens via lipopolysaccharides may be implicated (16, 19). Toutain et al. (56), however, suggest that rotation of *P. aeruginosa* is attributed to binding sites at the bacterium poles rather than along the body.

The distribution of each phenotype in the surface-associated population differed significantly depending on mutant type. Still, several general observations can be made for PAK bacteria attaching to the surface of the SCL. The rate of arrival to the surface was governed by convective diffusion. Attachment occurred through the flagellum, the pili, or the body. When any single attachment site was eliminated or disabled, the others could be substituted to provide sticking. In all cases studied here, there were at least two attachment sites available to the bacteria.

In all phenotypes, the percentage of fixed bacteria was a majority, typically over 50%. Our real-time observations occurred after 1 h of initial detection of bacteria at the lens surface. Presumably, the longer bacteria remain attached to the surface, the stronger they attach. If so, most attached bacteria evolve toward complete irreversible attachment. Interestingly, Singh et al. (50) found that for attached PAO1 bacteria under growth conditions, nearly 50% of the bacteria were squatters (stationary bacteria) in good comparison with our results. Surprisingly, despite using the same assay as that of Singh et al., Kirisits et al. (26) found few stationary wild-type PAO1 bacteria. We focused on initial binding of PAK under nongrowth conditions rather than early biofilms. For all phenotypes studied in our experiments, the fraction of detachment was small. However, it is possible that phenotypic changes in the attached population over longer times could permit dispersal from the lens (21).

For mutants without pili, but with an active flagellum (i.e., PAKΔ*pilA*), the fraction of surface-attached bacteria undergoing rotation increased significantly. For this class of mutant, it appeared that the fraction exhibiting twitching motility was replaced by one exhibiting rotation. Since nonpiliated mutants can rotate about their bodies, surface attachment in this case was via an adhesive site other than pili.

Since PAK exhibits body attachment sites other than pili, this suggests initial binding by the body, followed by pilus-propelled motion along the surface. Such a mechanism has significant implications for biofilm formation. All else being equal, lateral motion at the surfaces of individual bacteria permits surface collisions and aggregation in support of the current biofilm formation model (53). However, if biofilm formation occurs primarily during growth at the surface, twitching motion hinders biofilm growth as progeny bacteria migrate away from the parent (50).

Assays performed in a well-defined flow field are necessary for understanding of bacterial adhesion to surfaces. Nonswimming mutants of *PAK* associated with the contact lens surface at a much lower rate than that of the swimming strains. Thus, the ability to swim enhanced the rate of arrival to the surface. Arrival rates, however, do not correlate with adherence effec-

tiveness, as illustrated by the results for wt *PAK* and PAKΔ*fliC*. We also found that direct visual observation and enumeration of surface-associating subpopulations were crucial for understanding mechanisms of binding. *P. aeruginosa* bound to the contact lens through three different adhesion sites. Prevention of *P. aeruginosa* attachment would require blockage of all three adhesive locations. Thus, development of antifouling agents cannot focus on overcoming only one of the binding sites. Examination of surface phenotypes seems requisite to understanding the behavior of possible antifoulants. Although our findings apply specifically only to *P. aeruginosa* strain PAK and its interaction with the O_2Optix SCL (and glass) surfaces, it is likely that other strains of *P. aeruginosa*, and other bacterial species with multiple appendages, display similar surface phenotypes on other contact lens surfaces.

ACKNOWLEDGMENTS

V.B.T. acknowledges funding from a National Science Foundation graduate fellowship. Unrestricted funds from Alcon Laboratories, Fort Worth, TX, are gratefully appreciated. This work was also supported by NIH grant EY011221 to S.M.J.F.

REFERENCES

1. **Arora, S. K., B. W. Ritchings, E. C. Almira, S. Lory, and R. Ramphal.** 1998. The *Pseudomonas aeruginosa* flagellar cap protein, FliD, is responsible for mucin adhesion. Infect. Immun. **66:**1000–1007.
2. **Barton, J. W., and R. M. Ford.** 1995. Determination of effective transport-coefficients for bacterial migration in sand columns. Appl. Environ. Microbiol. **61:**3329–3335.
3. **Berg, H. C.** 1993. Random walks in biology, expanded edition. Princeton University Press, Princeton, NJ.
4. **Borazjani, N., et al.** 2005. Inhibition of bacterial adherence to contact lens cases and soft contact lenses, including high dk continuous wear silicone hydrogels: a new and unique attribute of ReNu with MoistureLoc solution. Invest. Ophthalmol. Vis. Sci. **46:**2769.
5. **Bruinsma, G. M., H. C. van der Mei, and H. J. Busscher.** 2001. Bacterial adhesion to surface hydrophilic and hydrophobic contact lenses. Biomaterials **22:**3217–3224.
6. **Busscher, H. J., and H. C. van der Mei.** 2006. Microbial adhesion in flow displacement systems. Clin. Microbiol. Rev. **19:**127–141.
7. **Busscher, H. J., and A. H. Weerkamp.** 1987. Specific and nonspecific interactions in bacterial adhesion to solid substrata. FEMS Microbiol. Rev. **46:** 165–173.
8. **Chambers, D., et al.** 2005. Factors associated with infection by *Pseudomonas aeruginosa* in adult cystic fibrosis. Eur. J. Respir. Dis. **26:**651–656.
9. **Cheng, K. H., et al.** 1999. Incidence of contact-lens-associated microbial keratitis and its related morbidity. Lancet **354:**181–185.
10. **Chiang, P., and L. L. Burrows.** 2003. Biofilm formation by hyperpiliated mutants of *Pseudomonas aeruginosa*. J. Bacteriol. **185:**2374–2378.
11. **Choo, J. D., B. A. Holden, E. B. Papas, and M. D. P. Willcox.** 2009. Adhesion of *Pseudomonas aeruginosa* to orthokeratology and alignment lenses. Optom. Vis. Sci. **86:**93–97.
12. **Choy, M. H., F. Stapleton, M. D. P. Willcox, and H. Zhu.** 2008. Comparison of virulence factors in *Pseudomonas aeruginosa* strains isolated from contact lens- and non-contact lens-related keratitis. J. Med. Microbiol. **57:**1539–1546.
13. **Comolli, J. C., et al.** 1999. *Pseudomonas aeruginosa* gene products PilT and PilU are required for cytotoxicity in vitro and virulence in a mouse model of acute pneumonia. Infect. Immun. **67:**3625–3630.
14. **Dasgupta, N., et al.** 2003. A four-tiered transcriptional regulatory circuit controls flagellar biogenesis in *Pseudomonas aeruginosa*. Mol. Microbiol. **50:**809–824.
15. **de Kerchove, A. J., and M. Elimelech.** 2007. Impact of alginate conditioning film on deposition kinetics of motile and nonmotile *Pseudomonas aeruginosa* strains. Appl. Environ. Microbiol. **73:**5227–5234.
16. **Fletcher, E. L., S. M. J. Fleiszig, and N. A. Brennan.** 1993. Lipopolysaccaride in adherence of *Pseudomonas aeruginosa* to corena and contact-lenses. Invest. Ophthalmol. Vis. Sci. **34:**1930–1936.
17. **Fletcher, E. L., et al.** 1993. The role of pili in the attachment of *Pseudomonas aeruginosa* to unworn hydrogel contact lenses. Curr. Eye Res. **12:**1067–1071.
18. **Garcia-Saenz, M. C., A. Arias-Puente, M. J. Fresnadillo-Martinez, and B. Paredes-Garcia.** 2002. Adherence of two strains of *Staphylococcus epidermidis* to contact lenses. Cornea **21:**511–515.
19. **Gupta, S. K., R. S. Berk, S. Masinick, and L. D. Hazlett.** 1994. Pili and lipopolysaccharide of *Pseudomonas aeruginosa* bind to glycolipid asialo gm1. Infect. Immun. **62:**4572–4579.
20. **Hahn, H. P.** 1997. The type-4 pilus is the major virulence-associated adhesin of *Pseudomonas aeruginosa*—a review. Gene **192:**99–108.
21. **Harmsen, M., L. A. Yang, S. J. Pamp, and T. Tolker-Nielsen.** 2010. An update on *Pseudomonas aeruginosa* biofilm formation, tolerance, and dispersal. FEMS Immunol. Med. Microbiol. **59:**253–268.
22. **Hazlett, L. D., and X. L. Rudner.** 1994. Investigations on the role of flagella in adhesion of *Pseudomonas aeruginosa* to mouse and human corneal epithelial. Ophthalmic Res. **26:**375–379.
23. **Henriques, M., et al.** 2005. Adhesion of *Pseudomonas aeruginosa* and *Staphylococcus epidermidis* to silicone-hydrogel contact lenses. Optom. Vis. Sci. **82:**446–450.
24. **Jenkins, A. T. A., R. Ffrench-Constant, A. Buckling, D. J. Clarke, and K. Jarvis.** 2004. Study of the attachment of *Pseudomonas aeruginosa* on gold and modified gold surfaces using surface plasmon resonance. Biotechnol. Prog. **20:**1233–1236.
25. **Keay, L., et al.** 2006. Microbial keratitis—predisposing factors and morbidity. Ophthalmology **113:**109–116.
26. **Kirisits, M. J., L. Prost, M. Starkey, and M. R. Parsek.** 2005. Characterization of colony morphology variants isolated from *Pseudomonas aeruginosa* biofilms. Appl. Environ. Microbiol. **71:**4809–4821.
27. **Klausen, M., et al.** 2003. Biofilm formation by *Pseudomonas aeruginosa* wild type, flagella and type IV pili mutants. Mol. Microbiol. **48:**1511–1524.
28. **Kodjikian, L., et al.** 2008. Bacterial adhesion to conventional hydrogel and new silicone-hydrogel contact lens materials. Graefes Arch. Clin. Exp. Ophthalmol. **246:**267–273.
29. **Lakkis, C., and S. M. Fleiszig.** 2001. Resistance of *Pseudomonas aeruginosa* isolates to hydrogel contact lens disinfection correlates with cytotoxic activity. J. Clin. Microbiol. **39:**1477–1486.
30. **Laroche, L., F. Thomas, C. Chaumeil, V. Borderie, and T. Bourcier.** 2003. Bacterial keratitis: predisposing factors, clinical and microbiological review of 300 cases. Invest. Ophthalmol. Vis. Sci. **44:**4764.
31. **Lévêque, M. A.** 1928. Les lois de la transmission de chaleur par convection. Ann. Mines Mem. Ser. **13:**201–299.
32. **Lillehoj, E. P., B. T. Kim, and K. C. Kim.** 2002. Identification of *Pseudomonas aeruginosa* flagellin as an adhesin for Muc1 mucin. Am. J. Physiol. Lung Cell. Mol. Physiol. **282:**L751–L756.
33. **Lira, M., L. Santos, J. Azeredo, E. Yebra-Pimentel, and M. Oliveira.** 2008. Comparative study of silicone-hydrogel contact lenses surfaces before and after wear using atomic force microscopy. J. Biomed. Mater. Res. B Appl. Biomater. **85:**361–367.
34. **Lok, B. K., Y. L. Cheng, and C. R. Robertson.** 1983. Protein adsorption on crosslinked polydimethlsiloxane using total internal-reflection fluorescence. J. Colloid Interface Sci. **91:**104–116.
35. **Lopez-Alemany, A., V. Compan, and M. F. Refojo.** 2002. Porous structure of Purevision (TM) versus Focus (R) night & day (TM) and conventional hydrogel contact lenses. J. Biomed. Mater. Res. **63:**319–325.
36. **Lyczak, J. B., C. L. Cannon, and G. B. Pier.** 2000. Establishment of *Pseudomonas aeruginosa* infection: lessons from a versatile opportunist. Microbes Infect. **2:**1051–1060.
37. **Marshall, K. C., R. Stout, and R. Mitchell.** 1971. Mechanism of initial event in sorption of marine bacteria to surfaces. J. Gen. Microbiol. **68:**337–348.
38. **Mattick, J. S.** 2002. Type IV pili and twitching motility. Annu. Rev. Microbiol. **56:**289–314.
39. **McClaine, J. W., and R. M. Ford.** 2002. Reversal of flagellar rotation is important in initial attachment of *Escherichia coli* to glass in a dynamic system with high- and low-ionic-strength buffers. Appl. Environ. Microbiol. **68:**1280–1289.
40. **Merz, A. J., M. So, and M. P. Sheetz.** 2000. Pilus retraction powers bacterial twitching motility. Nature **407:**98–102.
41. **Miller, M. J., and D. G. Ahearn.** 1987. Adherence of *Pseudomonas aeruginosa* to hydrophillic contact lenses and other substrata. J. Clin. Microbiol. **25:**1392–1397.
42. **Morgan, P. B., et al.** 2005. Risk factors for the development of corneal infiltrative events associated with contact lens wear. Invest. Ophthalmol. Vis. Sci. **46:**3136–3143.
43. **Mun, J. J., et al.** 2009. Clearance of *Pseudomonas aeruginosa* from a healthy ocular surface involves surfactant protein D and is compromised by bacterial elastase in a murine null-infection model. Infect. Immun. **77:**2392–2398.
44. **Newman, J., and K. Thomas-Alyew.** 2004. Electrochemical systems, 3rd ed., p. 377–415. Wiley Interscience, Hoboken, NJ.
45. **O'Toole, G. A., and R. Kolter.** 1998. Flagellar and twitching motility are necessary for *Pseudomonas aeruginosa* biofilm development. Mol. Microbiol. **30:**295–304.
46. **Ramphal, R., et al.** 1991. Adhesion of *Pseudomonas aeruginosa* pilin-deficient mutants to mucin. Infect. Immun. **59:**1307–1311.
47. **Ramphal, R., M. T. McNiece, and F. M. Polack.** 1981. Adherence of *Pseudomonas aeruginosa* to the injured cornea—a step in the pathogenesis of corneal infections. Ann. Ophthalmol. **13:**421–425.
48. **Santos, L., et al.** 2007. The effect of octylglucoside and sodium cholate in

Staphylococcus epidermidis and *Pseudomonas aeruginosa* adhesion to soft contact lenses. Optom. Vis. Sci. **84:**429–434.
49. **Silverman, M., and M. Simon.** 1974. Flagellar rotation and mechanisms of bacterial motility. Nature **249:**73–74.
50. **Singh, P. K., M. R. Parsek, E. P. Greenberg, and M. J. Welsh.** 2002. A component of innate immunity prevents bacterial biofilm development. Nature **417:**552–555.
51. **Sjoblad, R. D., and R. N. Doetsch.** 1982. Adsorption of polarly flagellated bacteria to bacteria surfaces. Curr. Microbiol. **7:**191–194.
52. **Skerker, J. M., and H. C. Berg.** 2001. Direct observation of extension and retraction of type IV pili. Proc. Natl. Acad. Sci. U. S. A. **98:**6901–6904.
53. **Stoodley, P., K. Sauer, D. G. Davies, and J. W. Costerton.** 2002. Biofilms as complex differentiated communities. Invest. Ophthalmol. Vis. Sci. **56:**187–209.
54. **Taylor, R. L., M. D. P. Willcox, T. J. Williams, and J. Verran.** 1998. Modulation of bacterial adhesion to hydrogel contact lenses by albumin. Optom. Vis. Sci. **75:**23–29.
55. **Thuruthyil, S. J., H. Zhu, and M. D. P. Willcox.** 2001. Serotype and adhesion of *Pseudomonas aeruginosa* isolated from contact lens wearers. Clin. Exp. Ophthalmol. **29:**147–149.
56. **Toutain, C. M., N. C. Caizza, M. E. Zegans, and G. A. O'Toole.** 2007. Roles for flagellar stators in biofilm formation by *Pseudomonas aeruginosa*. Res. Microbiol. **158:**471–477.
57. **Turner, L., W. S. Ryu, and H. C. Berg.** 2000. Real-time imaging of fluorescent flagellar filaments. J. Bacteriol. **182:**2793–2801.
58. **Vermeltfoort, P. B. J., et al.** 2006. Influence of day and night wear on surface properties of silicone hydrogel contact lenses and bacterial adhesion. Cornea **25:**516–523.
59. **Watson, A. A., J. S. Mattick, and R. A. Alm.** 1996. Functional expression of heterologous type 4 fimbriae in *Pseudomonas aeruginosa*. Gene **175:** 143–150.
60. **Whitchurch, C. B., and J. S. Mattick.** 1994. Characterization of a gene, pilU, required for twitching motility but not phage sensitivity in *Pseudomonas aeruginosa*. Mol. Microbiol. **13:**1079–1091.
61. **Willcox, M. D. P., and B. A. Holden.** 2001. Contact lens related corneal infections. Biosci. Rep. **21:**445–461.
62. **Zolfaghar, I., D. J. Evans, and S. M. J. Fleiszig.** 2003. Twitching motility contributes to the role of pili in corneal infection caused by *Pseudomonas aeruginosa*. Infect. Immun. **71:**5389–5393.